Hindawi Publishing Corporation
Journal of Nanomaterials
Volume 2010, Article ID 191058, 5 pages
doi:10.1155/2010/191058

Research Article

Low-Temperature Synthesis of Superconducting Nanocrystalline MgB_2

Jun Lu,[1,2] Zhili Xiao,[1,2] Qiyin Lin,[2] Helmut Claus,[2] and Zhigang Zak Fang[3]

[1] *Department of Physics, Northern Illinois University, DeKalb, IL 60115, USA*
[2] *Material Science Division, Argonne National Laboratory, Argonne, IL 60439, USA*
[3] *Department of Metallurgical Engineering, University of Utah, Salt Lake City, UT 84112, USA*

Correspondence should be addressed to Zhili Xiao, xiao@anl.gov

Received 14 October 2010; Accepted 31 December 2010

Academic Editor: Xuedong Bai

Magnesium diboride (MgB_2) is considered a promising material for practical application in superconducting devices, with a transition temperature near 40 K. In the present paper, nanocrystalline MgB_2 with an average particle size of approximately 70 nm is synthesized by reacting $LiBH_4$ with MgH_2 at temperatures as low as 450°C. This synthesis approach successfully bypasses the usage of either elemental boron or toxic diborane gas. The superconductivity of the nanostructures is confirmed by magnetization measurements, showing a superconducting critical temperature of 38.7 K.

1. Introduction

The discovery of superconductivity in binary metallic boride, MgB_2, with a transition temperature near 40 K has promoted a new interest in the area of fundamental and applied research on superconducting materials [1–6]. Considering its high critical temperature (high-T_c) coupled with the advantages of a large superconducting coherence length (5 nm) [7], weak-link-free grain boundaries [2], high critical current density in the range of 4–20 K, and large energy gap [8], MgB_2 is a promising material for practical applications in superconducting devices.

Traditionally, solid-state synthesis routes can be employed for the preparation of crystals, thin films, macroscopic wires, and tapes of this material. For instance, Canfield et al. [6] produced the first MgB_2 wires by diffusion of magnesium vapor into boron fibers reinforced by a tungsten core that exhibited inductive self-field J_c value of 10^5 A/cm^2 at 4.2 K. Although the solid-state synthesis method using elemental Mg and B has been successful in producing bulk MgB_2 phase, high temperatures (>800°C) are needed to complete the reaction. The reason for the need of high temperature has been suggested to be the general chemical inertness of boron, which may be due to the strong boron-boron bonds in elemental boron ($\Delta H_{B(s)\rightarrow B(g)}$ = 560 kJ/mol) [9]. Except for the high temperature, there are two other concerns of this approach to synthesize MgB_2 phase. On one hand, the high reactivity of Mg towards O_2 at elevated temperatures requires these reactions to be performed under carefully controlled conditions, considering that doping or contamination of the MgB_2 phase affects the superconducting transition temperature. On the other hand, the high volatility of Mg compared to that of B makes it difficult to control the stoichiometry and morphology of the product. On an attempt to produce MgB_2 one-dimensional (1D) nanostructures, M. Nath and B. A. Parkinson [10] successfully prepared MgB_2 nanowires and nanohelices by using diborane gas as a boron source at high temperatures. However, application of this approach is severely limited by the toxicity of diborane gas. It should be also noted that there are few reports on synthesis of nanostructured MgB_2 by using a solution-based methods [11, 12]. There, postannealing at high temperatures under diborane gas is still required to obtain nanocrystalline MgB_2. Therefore, finding a low-temperature and safe method to synthesize nanostructures of superconducting MgB_2 remains a challenge.

Herein we report the synthesis of superconducting nanocrystalline MgB_2 by the reaction of $LiBH_4$ with MgH_2 for the first time, according to the following reaction, which

takes place at the temperature range of 350–450°C:

$$LiBH_4 + \frac{1}{2}MgH_2 \longrightarrow LiH + \frac{1}{2}MgB_2 + 2H_2 \quad (1)$$

This approach successfully bypasses the usage of either elemental boron or toxic diborane gas. The superconductivity of the synthesized MgB_2 is confirmed by magnetization measurements.

2. Experimental Methods

The chemicals, MgH_2 and $LiBH_4$ powders, were purchased from Sigma-Aldrich Chemical Co. The purity of the reagent grade $LiBH_4$ was 99.9%. The MgH_2 powder was 95% pure and had particle size of 177~420 μm (40~80 mesh). Both chemicals are reactive with air and moisture. Therefore, they were stored and handled in an ultrahigh purity Argon (99.999%) filled glove box with <1 ppm oxygen and water concentrations.

In a typical experiment, 2.64 g of $LiBH_4$ powder was mixed with 1.56 g MgH_2 powder. To enhance the dehydrogenation kinetics, 4wt% $TiCl_3$ was added to the mixture according to [13]. This mixture was milled for 1 hour in a stainless steel milling vessel with 50 stainless steel milling balls (1/4 inch in diameter) using a commercial SPEX milling device. The mixture was then placed in a stainless-steel crucible, which was transferred to a sealed autoclave in the glove box. The autoclave was vacuumed to 10^{-3} bar by a mechanical pump which helps to enhance the dehydration reaction through reaction (1) according to [14]. Then, the autoclave was heated to 400–450°C with the ramping rate of 1°C/min and kept at the desired temperature for 12 hours, during which the pressure inside the autoclave can be raised up to several bars due to the release of hydrogen gas. Finally, the products were collected and washed carefully with ethanol and water, followed by drying the sample in vacuum at room temperature for 10 hours.

The identification of reactants and products in the mixture before and after the heat treatment was carried out using a PANalytical X'pert PRO X'Celerator diffractometer using Cu Ka radiation (λ = 1.5406 Å). Each sample for XRD analysis was mounted on a glass slide and covered with a Kapton tape as a protective film in the glove box. The X-ray intensity was measured over diffraction angle 2θ from 20° to 80° with a scanning rate of 0.02°/s. It should be noted that the amorphous-like broad peak around 20° is background signal from Kapton tape that was used to cover the powders. Based on XRD peak broadening, the crystallite size and effective internal strain of sample were estimated using the Scherrer equation, as described in the following equation [15]:

$$D_{hkl} = \frac{0.89\lambda}{\beta(2\theta)\cos(\theta)} \quad (2)$$

where $\beta(2\theta)$ is full width at half-maximum (FWHM) of the pure diffraction peak in radians, λ is the wavelength of the X-rays (0.15406 nm), θ is the diffraction angle, and D_{hkl} is the average diameter of the crystallite.

A scanning electron microscope (SEM, TOPCON SM-300) coupled with Energy Dispersive Spectrometry (EDS) was employed to observe the morphology and estimate the particle size of the samples. The samples were protected from exposure to air during the transfer to the SEM sample chamber by a conductive tape applied in a glove box. To obtain more accurate estimates of the particle sizes and or crystallite sizes, a transmission electron microscope (TEM, CM300) with an accelerating voltage of 200 kV was employed. To prepare a specimen for TEM observations, a dilute suspension, which was obtained from the sample ultrasonically dispersed in ethanol for 5 min, was dropped onto a copper grid and dried. Magnetization measurements were performed in a noncommercial SQUID magnetometer [16]. The earth magnetic field is shielded by a μ-metal shield, yielding a remanent magnetic field of less than 10 mGauss. Magnetic fields up to 50 Gauss can be obtained with a Cu solenoid.

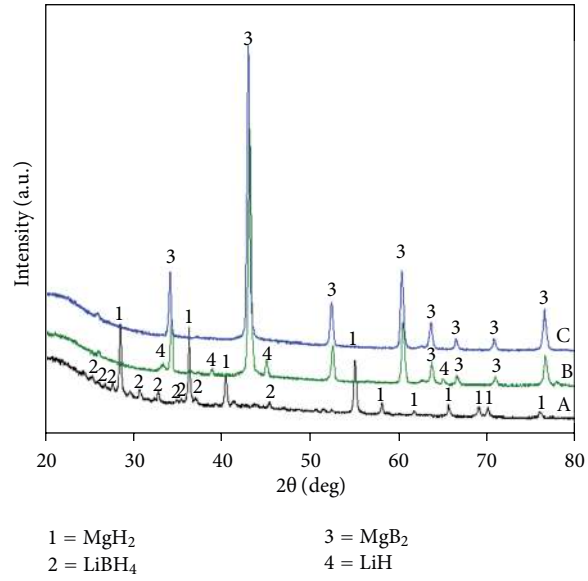

Figure 1: X-ray diffraction patterns from a mixture of $2LiBH_4 + MgH_2$ after milling (Curve A), dehydrogenation (Curve B), and purification (Curve C). The dehydrogenation temperature is 450°C; water and ethanol were used for purification.

3. Results and Discussion

In order to verify the completion of the reaction, X-ray diffraction (XRD) analysis was carried out on the raw materials as well as on the reaction products. Figure 1 shows the XRD patterns of a $2LiBH_4 + MgH_2$ mixture after mechanical milling, after dehydrogenation and after wash in water and ethanol. Crystalline phases are identified by comparing the experimental data with JCPDS files from the International Center for Diffraction Data. Curve A in Figure 1 shows the XRD pattern of sample after mechanical milling, in which the peaks marked with "1" are attributed to the tetragonal phase of MgH_2 and those marked with "2" are attributed to the phase of $LiBH_4$. No other diffraction was observed, indicating that mechanical milling only produced a physical

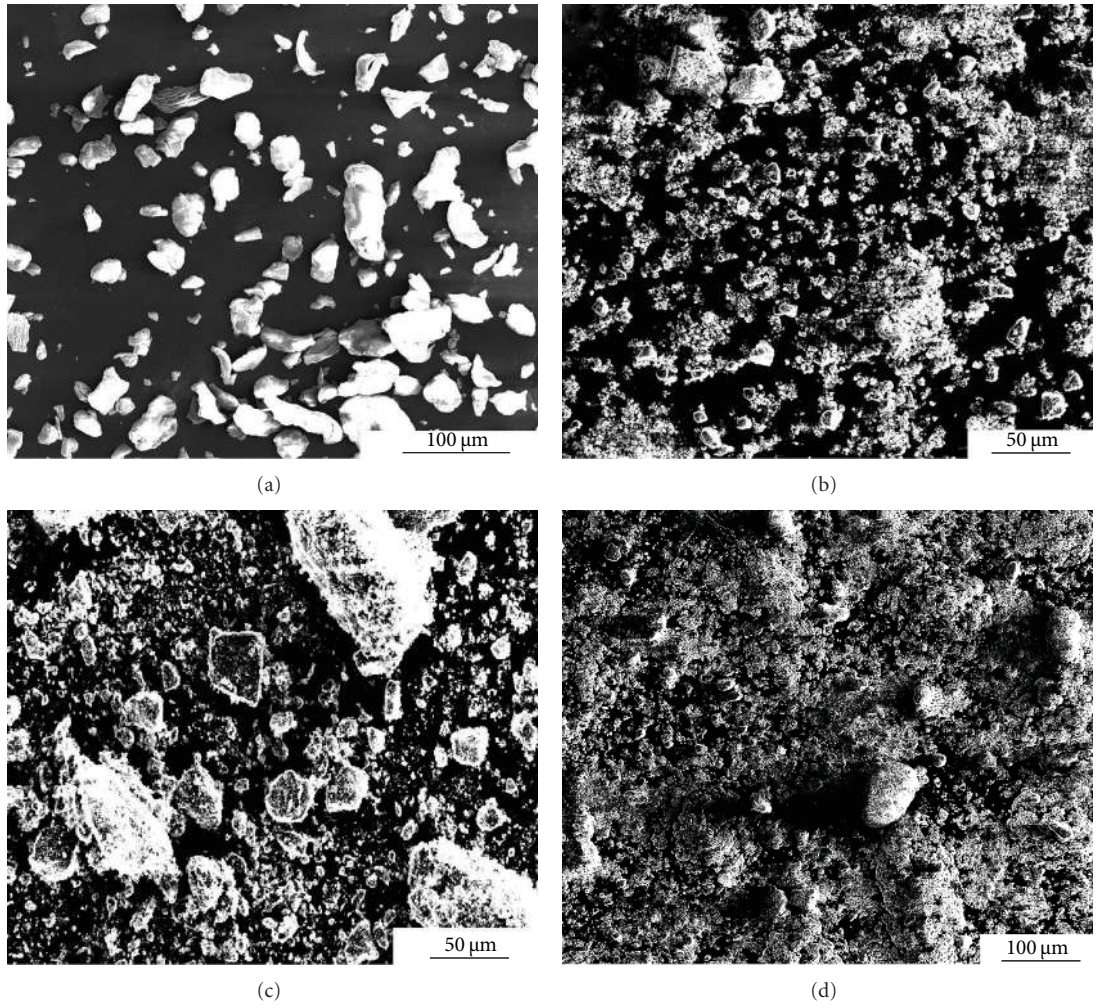

Figure 2: SEM images of (a) mixture of commercial MgH_2 and $LiBH_4$ powders, (b) mixture of MgH_2 and $LiBH_4$ after SPEX mill for 1 h, (c) mixture of MgH_2 and $LiBH_4$ after dehydrogenation at 450°C for 12 h, and (d) as-synthesized MgB_2 after purification.

mixture of $LiBH_4$ and MgH_2. Curve B in Figure 1 presents the XRD pattern of the sample after dehydrogenation at the temperature of 450°C, which clearly shows that $LiBH_4$ and MgH_2 phases are absent in the sample, indicating that they are consumed by the dehydrogenation and new compounds formed. The peaks marked with "3" are indexed to be the hexagonal phase of MgB_2, and those marked with "4" are indexed to be LiH. Thus, it can be concluded that according to the above XRD results the dehydrogenation of the mixture ($2LiBH_4 + MgH_2$) was carried out successfully at the above experimental conditions with the product being a mixture of MgB_2 + LiH. In order to separate MgB_2 from the mixture, a sequence of purification (the sample was washed by ethanol and water for several times, filtered out, and then dried in vacuum.) was performed, thanks to the reaction and solubility of LiH with water. The final product is indentified to be pure hexagonal MgB_2, as indicated by curve C in Figure 1. Based on (2), the average crystallite sizes of the obtained MgB_2 were calculated as about 70 nm, which is further confirmed by the TEM analysis as presented in Figure 3.

Scanning electron microscope (SEM) is used to study the particle sizes and morphologies of samples, as shown in Figure 2. The as-received MgH_2 and $LiBH_4$ powder is angular with an average particle size of around 150 μm (Figure 2(a)). After SPEX ball milling for 1 h, the average particle size (Figure 2(b)) has been reduced to the range of 5–20 μm, although some larger particles over 50 μm are still present. Figure 2(c) shows the SEM image of the sample after dehydrogenation at the temperature of 400°C, which indicates that the average particle size is in the range of 5–20 μm. Comparing Figure 2(b) and Figure 2(c), one can clearly see that there is little grain growth during the solid-state reaction at the temperature measured. It should be also noted that these values were much larger than those from XRD analyzer, mainly because the SEM only measure the particle size rather than the crystallite size, and the particles after milling were aggregated.

Transmission electron microscopy (TEM) image in Figure 3(a) shows that the as-prepared MgB_2 achieved after purification has an average particle size of about 80 nm,

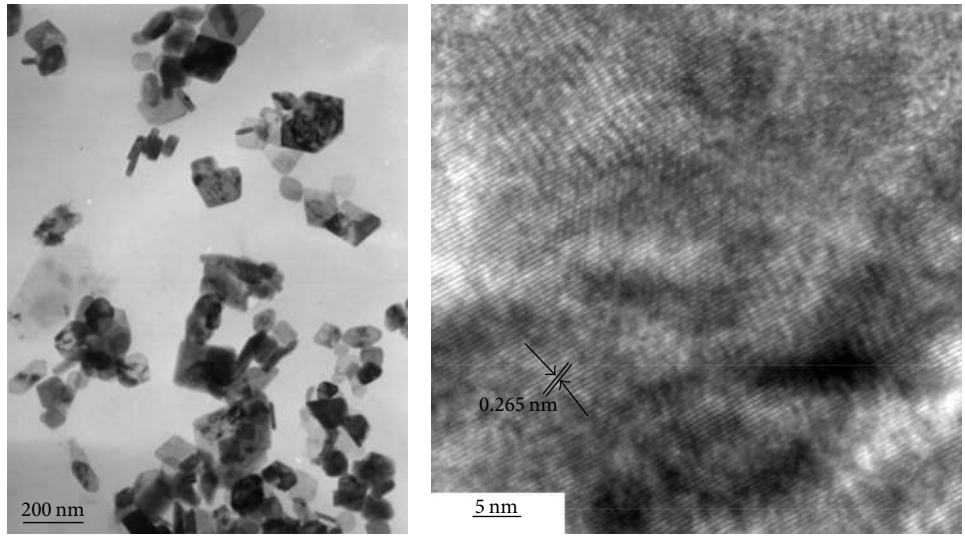

Figure 3: TEM images of the as-prepared MgB_2 particles. (a) Low-magnification TEM image showing nanostructures with size smaller than 100 nm. (b) High-magnification TEM image showing the lattice fringes.

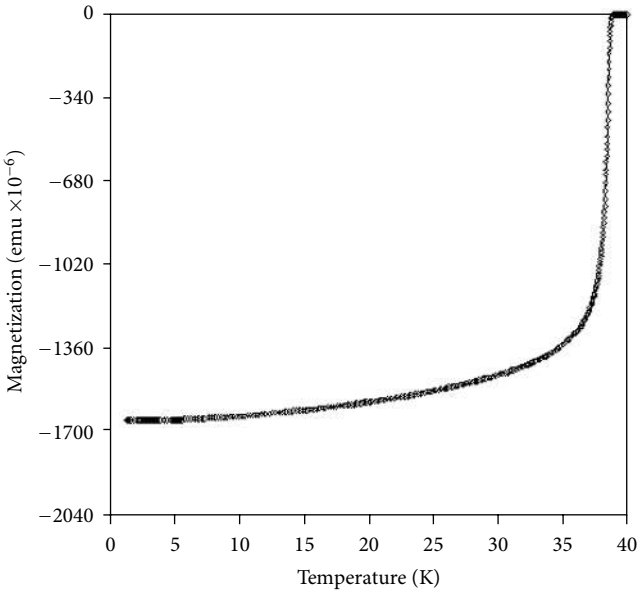

Figure 4: Magnetization of MgB_2 nanoparticles as function of temperature. Data were obtained under conditions of ZFC and 0.1 G.

which is close to that calculated from XRD patterns. Most of these particles are single crystal and show lattice fringes, as presented in the high-magnification TEM image in Figure 3(b). The layer separation estimated from the lattice fringes is approximately 2.56 Å, corresponding to the (100) spacing of the bulk MgB_2 (JCPDS files, card number 38-1369), indicating that the individual grain is crystalline.

Magnetization data on a powder sample from the dehydrogenated products of the mixture of Mg and $LiBH_4$ after washed with water and ethanol was collected using a noncommercial SQUID (superconducting quantum interface device) magnetometer [16]. The sample was zero-field-cooled (ZFC) from room temperature to 5 K, and the DC magnetization was then measured as a function of temperature under an applied field of 0.1 G. The observed shielding signal corresponded to full flux exclusion at low T. The onset of superconductivity was observed at about 38.7 K, as shown in Figure 4. It is interesting to note that T_c of the current sample is essentially the same as that of the bulk material. Considering that T_c in the MgB_2 system is generally sensitive to the presence of impurities, the above result suggests that MgB_2 powders produced from the current approach are chemically pure.

4. Conclusion

In summary, bulk quantities of nanostructured MgB_2 with an average particle size of approximately 70 nm have been successfully synthesized by reacting $LiBH_4$ with MgH_2 under the temperature as low as 450°C. The current approach successfully bypasses the usage of either elemental boron or toxic diborane gas. The superconductivity of the nanostructures is confirmed by magnetization measurement, showing a T_c of 38.7 K. These superconducting nanostructures can be potentially used as the building blocks in superconducting devices and as low dissipation interconnects in nanoscale electronics.

Acknowledgments

This work is supported by the US Department of Energy under Grant no. DE-FG02-06ER46334. The SEM and TEM analysis was performed at Argonne's Electron Microscopy Center (EMC) which is supported by DOE BES under contract no. DE-AC02-06CH11357.

References

[1] J. Nagamatsu, N. Nakagawa, T. Muranaka, Y. Zenitani, and J. Akimitsu, "Superconductivity at 39 K in magnesium diboride," *Nature*, vol. 410, no. 6824, pp. 63–64, 2001.

[2] D. C. Larbalestier, L. D. Cooley, M. O. Rikel et al., "Strongly linked current flow in polycrystalline forms of the superconductor MgB_2," *Nature*, vol. 410, no. 6825, pp. 186–189, 2001.

[3] D. G. Hinks, H. Claus, and J. D. Jorgensen, "The complex nature of superconductivity in MgB_2 as revealed by the reduced total isotope effect," *Nature*, vol. 411, no. 6836, pp. 457–460, 2001.

[4] W. N. Kang, H. J. Kim, E. H. Choi, C. U. Jung, and S. I. Lee, "MgB_2superconducting thin films with a transition temperature of 39 kelvin," *Science*, vol. 292, no. 5521, pp. 1521–1523, 2001.

[5] S. Jin, H. Mavoori, C. Bower, and R. B. van Dover, "High critical currents in iron-clad superconducting MgB_2 wires," *Nature*, vol. 411, no. 6837, pp. 563–565, 2001.

[6] P. C. Canfield, D. K. Finnemore, S. L. Bud'ko et al., "Superconductivity in dense MgB_2 wires," *Physical Review Letters*, vol. 86, no. 11, pp. 2423–2426, 2001.

[7] D. K. Finnemore, J. E. Ostenson, S. L. Bud'ko, G. Lapertot, and P. C. Canfield, "Thermodynamic and transport properties of superconducting MgB_2," *Physical Review Letters*, vol. 86, no. 11, pp. 2420–2422, 2001.

[8] S. Tsuda, T. Yokoya, T. Kiss et al., "Evidence for a multiple superconducting gap in MgB_2 from high-resolution photoemission spectroscopy," *Physical Review Letters*, vol. 87, no. 17, Article ID 177006, pp. 177006-1–177006-4, 2001.

[9] S. Orimo, Y. Nakamori, G. Kitahara et al., "Dehydriding and rehydriding reactions of $LiBH_4$," *Journal of Alloys and Compounds*, vol. 404-406, pp. 427–430, 2005.

[10] M. Nath and B. A. Parkinson, "Superconducting MgB_2 nanohelices grown on various substrates," *Journal of the American Chemical Society*, vol. 129, no. 37, pp. 11302–11303, 2007.

[11] M. Nath and B. A. Parkinson, "A simple sol-gel synthesis of superconducting MgB_2 nanowires," *Advanced Materials*, vol. 18, no. 14, pp. 1865–1868, 2006.

[12] A. K. Jha and N. Khare, "Single-crystalline superconducting MgB_2 nanowires," *Superconductor Science and Technology*, vol. 22, no. 7, Article ID 075017, 2009.

[13] E. Deprez, A. Justo, T. C. Rojas et al., "Microstructural study of the $LiBH_4$-MgH_2 reactive hydride composite with and without Ti-isopropoxide additive," *Acta Materialia*, vol. 58, no. 17, pp. 5683–5694, 2010.

[14] B. Bogdanović and M. Schwickardi, "Ti-doped alkali metal aluminium hydrides as potential novel reversible hydrogen storage materials," *Journal of Alloys and Compounds*, vol. 253-254, pp. 1–9, 1997.

[15] G. K. Williamson and W. H. Hall, "X-ray line broadening from filed aluminium and wolfram," *Acta Metallurgica*, vol. 1, no. 1, pp. 22–31, 1953.

[16] K. G. Vandervoort, G. Griffith, H. Claus, and G. W. Crabtree, "A low field SQUID magnetometer system for magnetic characterization of high-T superconducting samples," *Review of Scientific Instruments*, vol. 62, no. 9, pp. 2271–2275, 1991.